



# Lawrence Berkeley Laboratory

UNIVERSITY OF CALIFORNIA

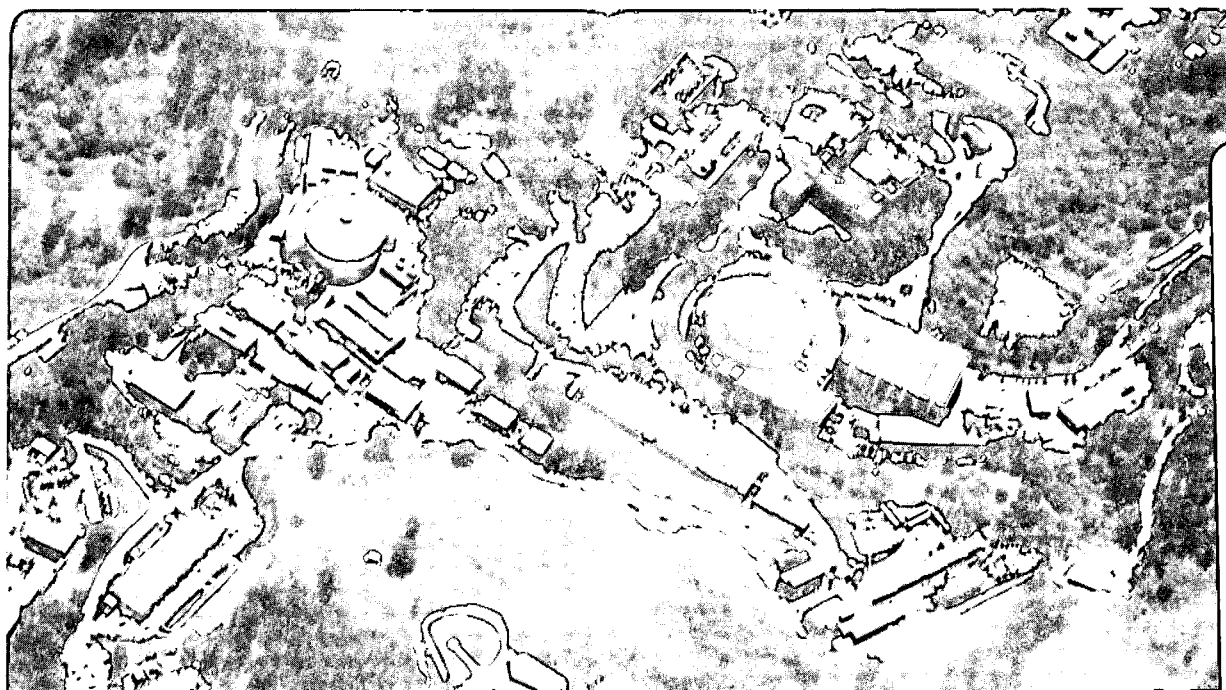
## Physics Division

Presented at the II International Conference on Calorimetry  
in High Energy Physics, Capri, Italy, October 14-18, 1991,  
and to be published in the Proceedings

### Test Beam Results from the D0 End Electromagnetic Calorimeter

N.A. Roe

November 1991



1 LOAN COPY 1  
1 Circulates 1  
1 for 4 weeks 1 Bldg. 50 Library.  
Copy 2

LBL-31497

#### DISCLAIMER

This document was prepared as an account of work sponsored by the United States Government. Neither the United States Government nor any agency thereof, nor The Regents of the University of California, nor any of their employees, makes any warranty, express or implied, or assumes any legal liability or responsibility for the accuracy, completeness, or usefulness of any information, apparatus, product, or process disclosed, or represents that its use would not infringe privately owned rights. Reference herein to any specific commercial product, process, or service by its trade name, trademark, manufacturer, or otherwise, does not necessarily constitute or imply its endorsement, recommendation, or favoring by the United States Government or any agency thereof, or The Regents of the University of California. The views and opinions of authors expressed herein do not necessarily state or reflect those of the United States Government or any agency thereof or The Regents of the University of California and shall not be used for advertising or product endorsement purposes.

Lawrence Berkeley Laboratory is an equal opportunity employer.

## **DISCLAIMER**

This document was prepared as an account of work sponsored by the United States Government. While this document is believed to contain correct information, neither the United States Government nor any agency thereof, nor the Regents of the University of California, nor any of their employees, makes any warranty, express or implied, or assumes any legal responsibility for the accuracy, completeness, or usefulness of any information, apparatus, product, or process disclosed, or represents that its use would not infringe privately owned rights. Reference herein to any specific commercial product, process, or service by its trade name, trademark, manufacturer, or otherwise, does not necessarily constitute or imply its endorsement, recommendation, or favoring by the United States Government or any agency thereof, or the Regents of the University of California. The views and opinions of authors expressed herein do not necessarily state or reflect those of the United States Government or any agency thereof or the Regents of the University of California.

**TEST BEAM RESULTS FROM THE D0 END  
ELECTROMAGNETIC CALORIMETER<sup>1</sup>**

Natalie A. Roe

Lawrence Berkeley Laboratory  
University of California  
Berkeley, CA 94720

November 1991

---

<sup>1</sup>This work was supported by the Director, Office of Energy Research, Office of High Energy and Nuclear Physics, Division of High Energy Physics of the U.S. Department of Energy under Contract DE-AC03-76SF00098.

# TEST BEAM RESULTS FROM THE D0 END ELECTROMAGNETIC CALORIMETER

NATALIE A. ROE†

*Lawrence Berkeley Laboratory  
1 Cyclotron Road, Berkeley, California 94720*

Representing the D0 Collaboration

## ABSTRACT

Test beam results are presented for the D0 end electromagnetic calorimeter. Data were taken with electrons and pions ranging in energy from 5 GeV to 150 GeV. Results from the analysis of the test beam data are presented on energy resolution and linearity, stability and uniformity of response, position resolution and electron-pion separation.

## 1. Introduction

D0 is a large multi-purpose detector located at Fermi National Accelerator Laboratory, on the Tevatron  $p\bar{p}$  Collider. The uranium-liquid argon calorimeter system of the D0 detector is comprised of two end calorimeters and a central calorimeter. Each of these three calorimeters contains an electromagnetic section with thin (3 or 4 mm) uranium plates, a fine hadronic section with thicker (6 mm) uranium plates, and a coarse hadronic section with thick (46 mm) copper or stainless steel plates. This contribution describes test beam measurements of an electromagnetic end calorimeter module (ECEM)<sup>1</sup> from the D0 detector.

### 1.1 Calorimeter Construction

In order to minimize energy losses and non-uniformities which arise in inter-modular cracks, the end electromagnetic calorimeters in the D0 detector feature a monolithic design in which the signal boards and uranium absorber plates are large disks of approximately 1 m radius. The basic sampling cell in the ECEM module consists of a 4 mm depleted uranium absorber plate, a 2.3 mm liquid argon gap, a 4.3 mm NEMA G-10 multilayer printed circuit signal board, and a second 2.3 mm liquid argon gap. The signal disks are constructed from five-layer printed circuit boards laminated with facesheets coated with a high resistivity epoxy. The resistive coat is maintained at positive high voltage to provide the drift field and the ionization charge drifting in the gap induces a signal on the pads.

---

† This work was supported by the Director, Office of Energy Research of the U.S. Department of Energy under Contract No. DE-AC03-76SF000098

The ECEM contains 18 sampling cells in depth, for a total of 20.1 radiation lengths ( $X_0$ ) of material at normal incidence. The signals from the 18 cells are ganged into four separate longitudinal depth segments consisting of 2, 2, 6 and 8 cells each. The longitudinal segmentation of the ECEM provides information about the longitudinal development of the electromagnetic shower and is valuable in distinguishing electrons from charged pions. The ECEM module is followed by a fine end calorimeter hadronic module<sup>2</sup> (ECIH) which contains a total of 7.3 interaction lengths, divided into five longitudinal sections.

Transverse segmentation in both modules is provided by the segmented copper readout pads on the signal boards, with each tower corresponding to an  $\eta \times \phi$  interval of  $0.1 \times 0.1$ .<sup>†</sup> In the third longitudinal section of the ECEM, which contains typically 65% of the electromagnetic shower energy, the transverse segmentation is doubled in both directions to  $0.05 \times 0.05$  in order to provide better shower position resolution for electrons. The segmented pads in both the ECEM and the ECIH are arranged in a semi-projective tower geometry.

### 1.2 Test Beam Setup

The D0 end calorimeter configuration was tested in the Neutrino-West beamline at Fermilab. The ECEM module was located in front of the ECIH module, and both modules were immersed in liquid argon inside a testbeam cryostat which had a thin window consisting of two 1.6 mm steel plates. A liquid argon excluder located between the cryostat window and the ECEM module was constructed of Rohacell slabs; it contained a 2.5 cm thick stainless steel plate, to simulate the D0 endcap cryostat wall, and a 4.4 cm thick aluminum plate at low angles, to simulate the material in the D0 vertex detector. The entire cryostat was located on a transporter under computer control, allowing the calorimeter response to be studied over the full range in  $\eta$  and over  $\pm 15^\circ$  in azimuthal angle.

The calorimeters were instrumented with the D0 electronic readout system<sup>3</sup> over a region of  $\approx 35^\circ$  in azimuth and over the full region in  $\eta$ ; in addition, a border region was instrumented in which groups of channels were ganged together. This allowed the energy flow out of the fully instrumented region to be monitored, while keeping the total channel count low.

Scintillators in the beam line provided the trigger, and PWC's located before and after the final bend magnet measured particle momenta (to 0.2%) and trajectories. Both pions and electrons were used, with momenta ranging from 5 to 150 GeV/c and a typical momentum spread of 1.5%.

## 2. End Electromagnetic Calorimeter Results

The analysis of the ECEM data proceeded by first correcting for electronic pedestals and gains, which were measured once every eight hours and once per day, respectively. Next, the response was corrected for the temperature dependence of

---

<sup>†</sup> The pseudo-rapidity variable,  $\eta$ , is defined by  $\eta = -\ln \tan \theta/2$ , where  $\theta$  is the polar angle measured from the beamline, and  $\phi$  is the azimuthal angle.

the electronics (0.08%/°C), for runs where this information was available.<sup>†</sup> The spread in the beam momentum was then corrected for event-by-event using the momentum measured by the PWC system. The energy of electromagnetic showers was reconstructed by summing all four longitudinal sections in the ECEM and the first section of the ECIH. The number of towers summed to contain an electromagnetic shower varied with  $\eta$ , corresponding to the variation of tower size with  $\eta$ . For example, for  $\eta=1.95$  with towers of 5.2 cm square, 99.5% containment was achieved by summing an array of 5 by 5 towers, while at  $\eta = 2.5$  with towers of 2.8 cm square, an array of 9 by 9 towers was needed.

### 2.1 Energy Resolution and Linearity

To measure the total energy of an electromagnetic shower in the ECEM, relative weights for the signals from each longitudinal section must be determined. These weights correspond to the inverse of the relative sampling fractions (SF's), and were obtained by simultaneously minimizing the energy resolution and the deviation from linearity for electrons ranging from 10 to 150 GeV/c. The data for this analysis were all taken at  $\eta = 1.95$ , at the so-called benchmark spot. A single set of optimized SF's was found for all electron energies; these values are very similar to the relative SF's calculated from minimum ionizing dE/dX energy deposition. The energy resolution obtained with these weights is given by

$$\frac{\sigma_E}{E} = (0.0034 \pm .0019) \oplus \frac{(0.157 \pm 0.005)}{\sqrt{E}} \oplus \frac{(0.330 \pm 0.030)}{E}, \quad (1)$$

where the three contributions are, respectively, the constant (or calibration) term, the sampling term, and the noise term (which is consistent with the measured noise), and all three terms are to be added in quadrature. The ECEM response was linear to within 0.2% over the energy range of 10 to 150 GeV.

### 2.2 Stability and Uniformity of Response

The temporal stability of the ECEM response was monitored by taking data with 100 GeV electrons at the benchmark spot ( $\eta=1.95$ ) at approximately daily intervals during the test beam run. Only data for which the temperature of the readout electronics was monitored were included in the analysis. A fit to the data showed a change in response of  $(-0.12 \pm 0.04)\%$  /40 days. If we assume this decrease is due to increasing oxygen contamination in the liquid argon, this would correspond to an increase of 0.013 ppm / 40 days,<sup>4</sup> to be compared to the measured effective oxygen content of 0.45 ppm.<sup>5</sup> The oxygen contamination of the liquid argon was independently monitored at the test beam with  $\alpha$  and  $\beta$  sources;<sup>6</sup> the results of those measurements are also consistent with a small increase in oxygen contamination during the test beam run.

To study the spatial uniformity of the ECEM response, we performed azimuthal scans of the module at  $\eta = 1.85$  and 1.95 with 100 GeV electrons. The mean pulse height as a function of azimuth is shown in Fig. 1 for  $\eta=1.85$ , where the azimuth

---

<sup>†</sup> The electronics temperature was monitored only during the last 40 days of the run.

is given as the arc length,  $s = \text{radius} \times \phi$ . The mean response is constant to within 0.5% (rms). Similar results were obtained at  $\eta = 1.95$  (0.5% rms). Small regions of non-uniform response near structural elements were also studied; these amount to less than 3.4% of the total area, and the maximum correction required is 15%.

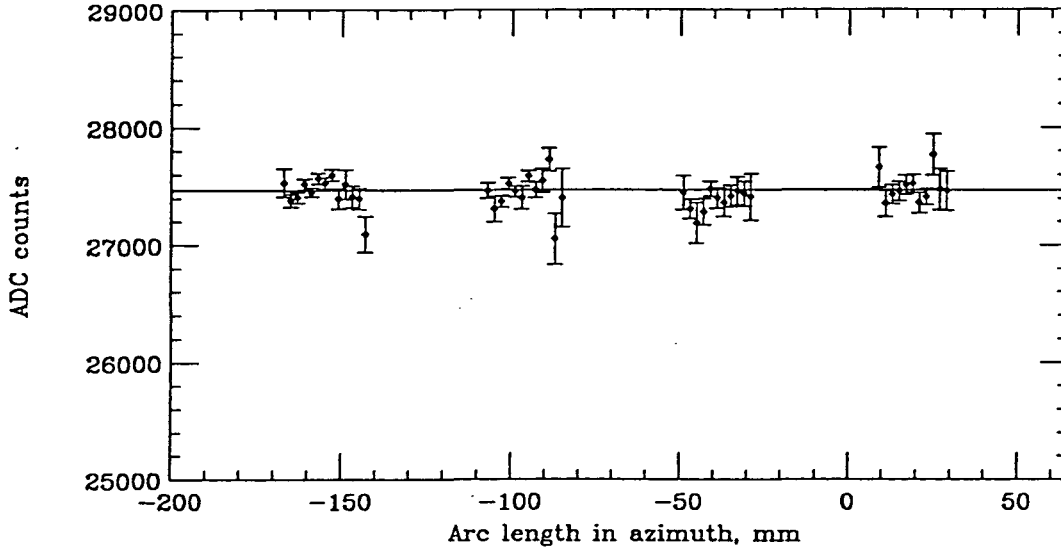


Fig. 1. ECEM response in ADC counts for azimuthal scan at  $\eta=1.85$ ; the rms is 0.5%.

### 2.3 Position Resolution

The centroid of an electromagnetic shower can be determined to much better accuracy than one would naively calculate based on the calorimeter segmentation, due to the transverse spread of the shower which results in sharing of the energy among several towers. In the ECEM, the shower position can be most accurately determined in the third longitudinal section (EM3), which has a transverse segmentation of  $.05 \times .05$  in  $\eta \times \phi$ . We have studied the position resolution in EM3 using the shower impact position extrapolated from the PWC's in the beamline. Several techniques are available to extract the impact point of an electromagnetic shower; we have studied two algorithms, both of which give very satisfactory results.

In the first method, the transverse shower shape is fit to the sum of two exponentials and a ratio of observed energies is constructed, from which the shower impact position can be iteratively determined.<sup>1,7</sup> In the second method,<sup>8</sup> a first estimate of the position is made by calculating the energy weighted center-of-gravity,  $X_{cog} = \sum X_i E_i / \sum E_i$ , and then correcting it with the following algorithm:

$$X_{ccog} = X_m + B \cdot \sinh^{-1} \left\{ \frac{(X_{cog} - X_m)}{\Delta} \cdot \sinh\left(\frac{\Delta}{B}\right) \right\}. \quad (2)$$

In this expression,  $X_m$  is the position of the EM3 tower with the maximum signal,  $\Delta$  is the pad half-width and  $B$  characterizes the transverse shower shape assuming a single exponential transverse shape.

The position resolution as determined by these two techniques was very similar. In both cases, the best resolution is obtained when the shower impacts near a tower edge, and gets worse as the square of the distance from the tower edge. In addition, due to the inherently statistical nature of shower development we expect the position resolution to vary approximately as  $1/\sqrt{E}$ . In Fig. 2 the position resolution obtained using the corrected center-of-gravity technique is shown as a function of energy. Both the resolution at the tower edge, and the resolution integrated over the tower width at  $\eta=1.95$  (where the pad size in EM3 is 2.6 cm) are shown. The former does vary approximately as  $1/\sqrt{E}$  while the average resolution shows a slightly steeper dependence. The average resolution is approximately 2 mm at 25 GeV and 1 mm at 75 GeV.

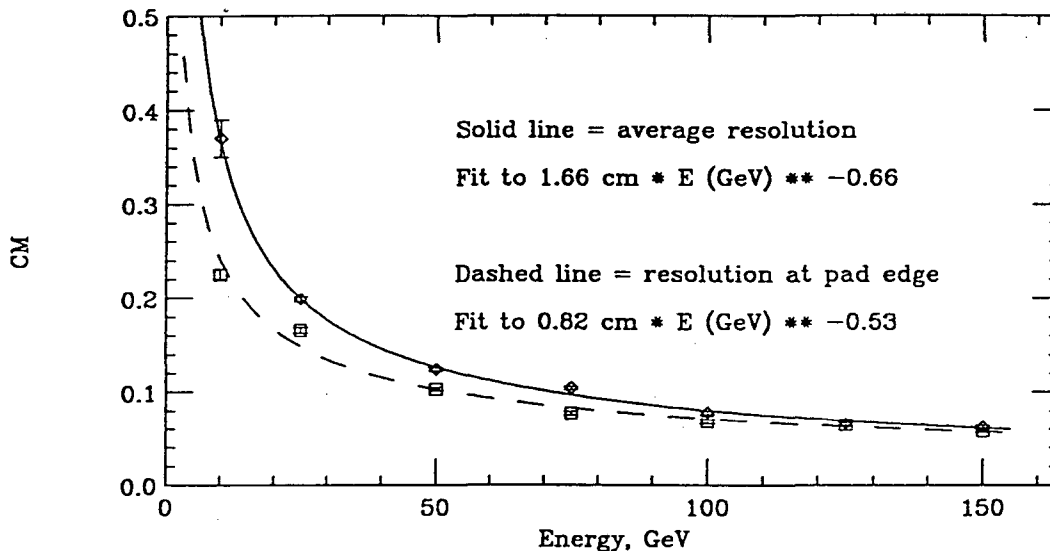


Fig. 2. Position resolution vs. energy for electrons incident at  $\eta=1.95$ .

#### 2.4 Electron-Pion Separation

The development of electron and pion showers is quite different, and the resulting difference in shower shape can be exploited to identify electrons and reject the larger background from pions. Both longitudinal and transverse shower shape variables can be used; in addition there are correlations which should be taken into account to maximize the pion rejection while retaining good electron efficiency.

We have used an H-matrix technique<sup>9</sup> to perform  $e/\pi$  separation. In this technique, a training sample of electrons is used to compute the mean energy deposited in each element along with the correlations to every other element. The inverse of this matrix is then used to compute an effective  $\chi^2$ , which we call  $\zeta$ ; a cut is then placed on the value of  $\zeta$  to separate electrons and pions. Two different H-matrices have been used: in the first, all signals in each longitudinal section of the ECEM and the first ECIH layer are individually summed to create a  $5 \times 5$  matrix; in the

second, all channels in each layer within a  $0.3 \times 0.3$  tower are used to create a  $72 \times 72$  matrix. The  $5 \times 5$  H-matrix only takes into account the difference in the longitudinal shower development while the  $72 \times 72$  H-matrix includes both longitudinal and transverse shower characteristics.

To obtain the best  $e/\pi$  separation, both H-matrices were applied sequentially. On an independent sample of electrons the  $\zeta$  cuts were chosen for an overall electron efficiency of 95%. The pion rejection was then determined by applying the same cuts to pion test beam data; the measurement is statistically limited so we quote a 95% C.L. lower limit on the pion rejection factor, of 700 at 50 GeV and  $2 \times 10^3$  at 100 GeV.

#### 4. Conclusions

Analysis of testbeam data from the D0 ECEM calorimeter module has been presented. The module has good energy resolution with a small constant term; is very linear, stable and uniform in response; has position resolution better than 1 mm for high energy electrons; and has an  $e/\pi$  rejection factor greater than 700 at 95% C.L., for energies greater than 50 GeV and an electron efficiency of 95%.

#### 5. Acknowledgements

We would like to thank the Fermilab Accelerator Division and the staffs of the collaborating institutions on D0 for their contributions to the success of this project. This work was supported by the Director, Office of Energy Research of the U.S. Department of Energy under Contract No. DE-AC03-76SF00098.

#### 6. References

1. See also H. Aihara, *et.al.*, *The Design, Construction and Performance of the D0 End Electromagnetic Calorimeter Module*, LBL-31378, to be submitted to NIM; H. Aihara, IEEE Trans. on Nuc. Sci **38** (1991) 398; and A.L. Spadafora, in *Proc. of the 1st Int'l Conf. on Calorimetry in High Energy Physics*, ed. Anderson *et.al.* (World Scientific, Singapore, 1991) p. 77.
2. N. A. Amos, in *Proc of the 1st Int'l Conf. on Calorimetry in High Energy Physics*, ed. Anderson *et.al.* (World Scientific, Singapore, 1991) p. 84.
3. M. Demarteau, in *Proc of the 1st Int'l Conf. on Calorimetry in High Energy Physics*, ed. Anderson *et.al.* (World Scientific, Singapore, 1991) p. 91.
4. H. Aihara and A. Allen, D0 Note # 1262, Oct. 1991 (unpublished).
5. A. Allen and A.L. Spadafora, D0 Note # 1212, Sept. 1991 (unpublished).
6. G. Blazey, in *Proc of the 1st Int'l Conf. on Calorimetry in High Energy Physics*, ed. Anderson *et.al.* (World Scientific, Singapore, 1991) p. 101.
7. M. Demarteau, D0 Note #842, May 1989 (unpublished).
8. G.A. Akopdjanov, *et.al.*, NIM **140** (1977) 441, and A. De Angelis and F. Mazzone, NIM **A287** (1990) 397.
9. R. Englemann *et.al.*, NIM **216** (1983) 45.

LAWRENCE BERKELEY LABORATORY  
UNIVERSITY OF CALIFORNIA  
INFORMATION RESOURCES DEPARTMENT  
BERKELEY, CALIFORNIA 94720